J Mater Sci (2007) 42:1336–1342
DOI 10.1007/s10853-006-1209-y

Negative Poisson's ratio structures produced from zirconia and nickel using co-extrusion

Aaron T. Crumm · John W. Halloran

Received: 16 November 2005 / Accepted: 20 January 2006 / Published online: 30 November 2006

Abstract Objects with a complex structure designed to display negative Poisson's ratio were produced from zirconia ceramic and from metallic nickel. The objects were arrays of repeat units with designed elastic behavior. The technique of microfabrication by coextrusion, based on oxide powders blended with thermoplastics, was used to replicate and miniaturize single 38 mm repeat unit to obtain an array of 64 units, 400 μm in size. The metallic nickel objects were produced fabricating nickel oxide, followed by sintering in a reducing atmosphere to yield dense metallic nickel. Poisson's ratio of the nickel structure was –0.3.

Introduction

Most materials have a positive Poisson's ratio, so they react to a tensile load by contracting laterally. There is increasing interest in materials which act conversely, namely materials that expand laterally when subjected to a tensile load and contract laterally when compressed. The only naturally occurring examples of materials with an isotropic negative Poisson's response are cork, which as Poisson's ratio value close to zero and aggregate crystals of α-cristobalite [1]. Some synthetic negative-Poisson's ratio materials include re-entrant structures, polymer foams, metal foams, and polymer chains altered at the molecular level. Re-entrant structures are reverse honeycomb like architectures with inverted walls such that an in-plane stress creates a negative Poisson's ratio effect in the orthogonal direction [2]. Foamed metals and polymers processed to impose a re-entrant geometry on their foam structure can have negative Poisson's ratios [3, 4]. Microporous polymers with negative Poisson's ratio have been created from polytetrafluoroethylene and ultra-high molecular weight polyethylene [5–8]. In all cases, the effect is produced by non-central forces acting to give a bi-directional displacement under the action of a unidirectional load. The advantages of negative Poisson's ratio materials include enhanced indentation resistance and plane strain fracture [3]. Potential applications of these materials include their use as sound deadening layers, enhanced modulus composites, and novel fasteners [9–11].

Regardless of the mechanism responsible for the negative Poisson's ratio behavior of the materials listed above, they share a strong non-linear strain response and a limited strain capacity [12, 13]. Ideally a negative Poisson's ratio material would have a linear response over a broad range strain. Recently, the topology optimization and homogenization method has been used to design ''artificial materials'' with unusual elastic properties including negative Poisson's ratio [14–16]. Figure 1 shows a design from Sigmund consisting of a repeat unit with beams and hinges designed to expand laterally in response to axial strains. When this is produced in an array of many units, it generates an ''artificial material'' with negative Poisson's ratio.

A. T. Crumm (✉) · J. W. Halloran
Department of Materials Science and Engineering, University of Michigan, 3062 Dow Building, Ann Arbor, MI 48109-2136, USA
e-mail: john_halloran@engin.umich.edu

Present Address:
A. T. Crumm
Adaptive Materials Incorporated, Ann Arbor, MI, USA

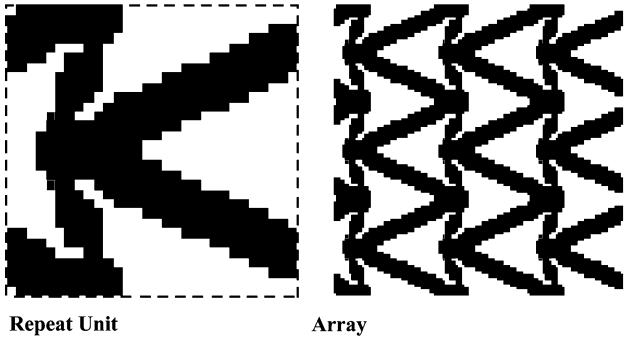

Fig. 1 Negative Poisson's ratio design by Sigmund [15], showing single repeat unit from Topology Optimization Design on left, and an array of units on the right

This design has a large negative linear response. The paper addresses the fabrication and properties of a structure based on this Sigmund design from nickel and zirconia.

Fabrication of negative Poisson's ratio structures

The Sigmund design has a two dimensional array of repeating units, and must be fabricated into bulk objects consisting of a large number of small units. To realize these, we adopt the technique of microfabrication by co-extrusion (MFCX) [17]. This technique uses compounds of ceramic powders with thermoplastic resins and exploits the idea that an extrusion ''feed rod'' with a centimeter-scale design can be reduced in size by forcing it through a reduction die. Further reductions can by achieved by assembling the first-stage extrudate, into a second feed rod, and repeating the extrusion. In this case there are two powder-thermoplastic compounds: Zirconia-thermoplastic for the ceramic regions and carbon black for the empty space regions. During firing, the carbon black oxidizes away, acting as a void-forming fugitive. Size reduction can be achieved without distortion of the design if the flow behavior of the two thermoplastic compounds is carefully matched. Rheological matching is achieved by adjusting the powder volume fraction, the viscosity of the base resin, as well as processing aids and surfactants unique to each powder-resin combination. The base resin for this work is an ethylene co-polymer based blend similar to previous reports [18].

Zirconia negative Poisson's ratio structure

Fifty volume percent of a commercial 3Y-TZP zirconia powder (3 mol% yttria stabilized, average particle size of 200 nm and a surface area of 5.2 m^2/gm surface area, Tosoh, Japan) was compounded with molten ethylene co-polymer using electrically heated, high intensity shear mixer (Brabender Corp, Model PL2100, USA) to produce a zirconia-thermoplastic compound. A fugitive compound was produced by similarly compounding carbon black powder (Black Pearls 120, Cabot USA, average particle size d_{50} = 75 nm, nitrogen surface area 25 m^2/g). The fugitive and zirconia compounds were compounded to equivalent apparent viscosity values of 2900 ± 150 Pa s at an apparent shear rate of 111 ± 4 s^{-1} and stock temperature of 125 ± 1 °C

The first step was to construct a single repeat unit of the Sigmund design from the zirconia compound and the fugitive compound. This is shown in Fig. 2. On the left is the cross-section of a 38-mm square feed rod assembled from these two compounds. The feed rod is about 100-mm long. The assembly was done by forming standard blocks, rods, and sheets of the zirconia material by warm-molding. These were inserted into cavities cut into a 38-mm square molded block of the black material, using ordinary carpentry saws and knives. The assembly is bonded into a solid object by uniaxially pressing at 11 MPa at 160 °C. The completed feed rod was coextruded using a piston drive device (Bradford University Research, Ltd, Bradford UK) at 115 °C and 3 mm/min through an 8:1 square symmetric reduction die. This produced a long extrudate 4.75-mm square, with the same design, but reduced in height by a factor of 8. Sixty-four lengths of extrudate from the first coextrusion pass were assembled into the second feed rod and bonded

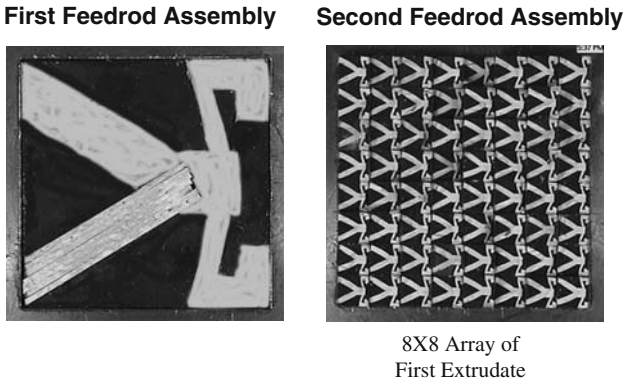

Fig. 2 Zirconia negative Poisson's ratio object feed rod assembly method Left: First feed rod assembled from slabs and blocks of zirconia-thermoplastic compound (white) in matrix of carbon black-thermoplastic compound (black). This was then extruded through an 8:1 reduction die Right: Second feed rod assembled as an 8 by 8 array of the first extrudate, after warm pressing. Both objects are 38 mm square

together to form a 38-mm square block. This block was sliced axially to produce 8-by–8 arrays of green zirconia units.

Sections sliced from the large-scale block were sintered. Binder burnout and fugitive removal were accomplished by thermally processing in a sealed tube furnace with a flowing atmosphere of air. The heating schedule was multi-step sequence of ramps and holds with slow heating in critical regions (5 °C/h between 250 °C and 325 °C) and faster heating in non-critical regions (120 °C/h between 600 °C and 900 °C). The thermoplastic binder was removed below 400 °C, providing a body that could be easily sintered. The carbon black fugitive was oxidized around 600 °C, and the space it occupied became the voids in the design. The binder free parts were transferred to a high temperature furnace and sintered to a pore free state by heating to 1375 °C at 5 °C/min and holding for 1 h.

A section of the sintered zirconia part, comprised of an array of 4 mm repeat units, is pictured in Fig. 3. The repeat units exhibited excellent shape retention. The unit cells had imperfect registration between neighboring unit cells, several struts had as much as a 50% reduction in their available contact area. The brittleness of the zirconia ceramic and the stress concentrations inherent in the sharp cornered architecture made it difficult to conclusively determine the Poisson's ratio response of this structure, so we made a metallic version.

Coextrusion of NiO and reductive sintering to Ni

We chose to use an easily reduced transition metal oxide, which could be processed as a fine ceramic powder, heated in air to remove the carbon black fugitive, and reduced during sintering in a hydrogen atmosphere. Iron oxide, copper oxide, and nickel oxide were found to work well. Nickel oxide was selected based on its ease of reduction thermodynamically, its high melting temperature, and its ready availability in powder form. Sintering in 10%H_2–90%N_2 provided a convenient atmosphere.

Before fabricating the negative Poisson's ratio architecture, it was necessary to determine how to transform a ceramic green body of nickel oxide powder into a dense metallic nickel part. Commercially obtained nickel oxide powder (99% NiO, –325 mesh, Alfa Aesar, USA) was ball milled in isopropanol with 1 wt% steric acid reduce the particle size and the surface of the powder for improved compounding and extrusion performance. The nickel oxide and carbon black fugitive powders were compounded with the molten thermoplastic at 55 vol% loading for the NiO and 41 vol% for the carbon black, to achieve an equivalent apparent viscosity value for both compounds of 3200 ± 150 Pa s at an apparent shear rate of 111 ± 4 s^{-1} and stock temperature of 119 ± 1 °C.

The nickel oxide and fugitive thermoplastic compounds were extruded into 4.7 mm square rods and sheets 1 mm thick using stainless steel extrusion dies at a ram rate of 3 mm/min and a die temperature of 115 °C. Samples of the coextrusion compounds were subjected to thermogravimetric analysis in a flowing air environment and a constant ramp rate of 2 °C/min to 800 °C, shown in Fig. 4. Both the fugitive and nickel oxide compounds exhibited binder burnout behaviors typical of organic system typically employed for MFCX. The nickel oxide compound exhibited a rapid organic weight loss between 190 °C and 390 °C followed by no weight change to 700 °C in flowing air. The fugitive compound exhibited a two staged weight loss curve representative of the separate removal of the organic vehicle and carbon black fugitive powder. The majority of the polymer (44 total wt%) is pyrolyzed between 190 °C and 400 °C. The majority of the carbon black fugitive powder is oxidized between 500 °C and 575 °C.

Samples that were previously pyrolyzed in air to 650 °C were used to determine the weight loss behavior during reduction in a 10%H_2/90%N_2 reducing atmosphere. The thermogravimetric results appear in

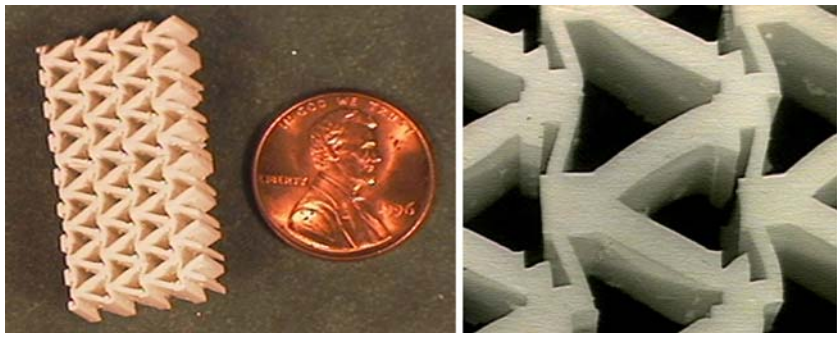

Fig. 3 Sintered zirconia negative Poisson's ratio architecture. Left: Section of sintered zirconia design with 32 repeat units Right: Detail of repeat units, showing 4 mm units with 340 μm minimum feature size

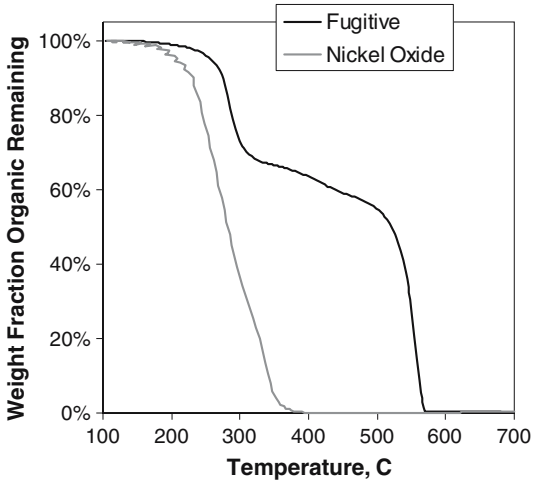

Fig. 4 Thermogravimetric analysis of nickel oxide and fugitive extrusion compounds in air

Fig. 5. The change in curvature that occurs in the nickel oxide reduction weight loss curve at ~400 °C signifies the transition into a regime where the diffusion flux of reactant gases is kinetically limited by the thickening porous reacted zone [19]. The nickel oxide is completely reduced by ~600 °C for a constant ramp rate of 1.5 °C/min in flowing 10%H_2/90%N_2.

It is well documented that low temperature portion of the thermal profile during reduction causes the oxide particles to form porous metallic sponge [19]. SEM examination of samples at various temperatures showed the evolution of the dense nickel oxide particles to oxide-metal sponge between ~400 °C and ~600 °C. Above 600 °C the nickel is completely reduced, and densification begins to occur. The formation of a metallic sponge is critical to the successful sintering of the final metallic part. The large shrinkage associated with molar volume change between nickel in its oxide and metal forms, 6.59 cm^3/mol and 11.12 cm^3/mol respectively, yields net volumetric shrinkage of 67.4% assuming an initial green density of nickel oxide compound of 55 vol%. The gradual transformation to a metallic sponge helps to spread the net shrinkage of the part across a broad temperature range. This phenomenon is captured in Fig. 6, showing the linear shrinkage curve generated for a set of samples subjected to a set of reduction temperatures. The samples begin to shrink at ~300 °C, which corresponds to the initial reduction weight loss observed during thermogravimetric analysis. Densification continues until the samples are fully densified at ~1,050 °C. The low temperature reduction processing of the nickel oxide results in a dramatically protracted sintering curve that spans ~750 °C. Samples of nickel oxide extrusion compound fired to 1,050 °C for 1 h in 10%H_2/90%N_2 had distributed porosity with average pore size of 0.45 μm (maximum observed 3 μm). The reduced nickel was 98.6% dense as determined by the standard Archimedes buoyancy technique. The final experimental linear shrinkage value of 31.9 ± 1.1% is in very close to the expected theoretical linear shrinkage of 31.2%.

The metal formed from the reduction of nickel oxide MFCX extrusion compounds was strong and ductile. Coupons of nickel were tested in tension on a hydraulically actuated machine (MTS System 810 Hydraulic Test Frame, USA) using test specimen fabricated from sheets of the coextrusion compound thermally processed in an identical manner as the negative Poisson ratio architectures. The sheet specimen measured 12.3 mm wide by 0.56 mm thick and

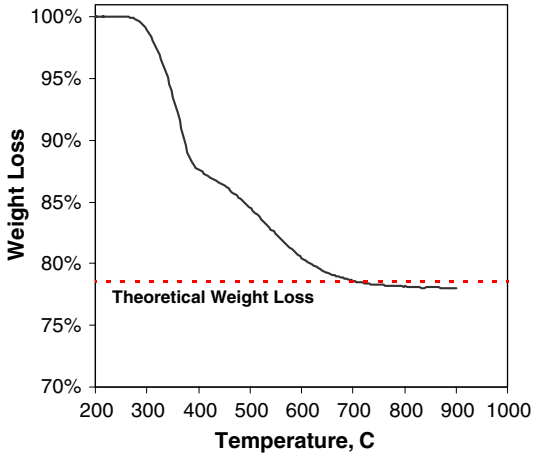

Fig. 5 Thermogravimetric analysis of nickel oxide reduction process in 10%H_2–90%N_2 at 90 °C/h ramp rate

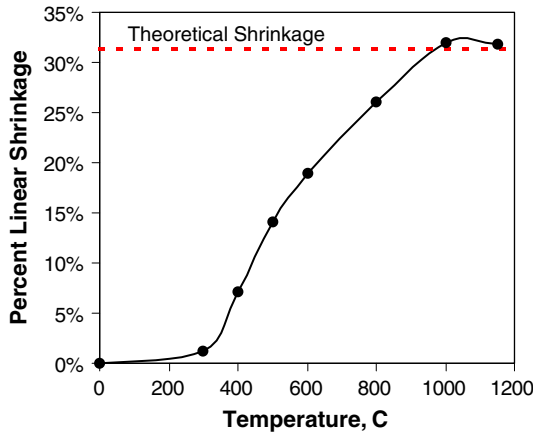

Fig. 6 Percent linear shrinkage of samples of binder-free nickel oxide extrusion compound during metallic reduction processing (90 °C/h ramp rate, flowing 10%H_2/90%N_2 reducing gas)

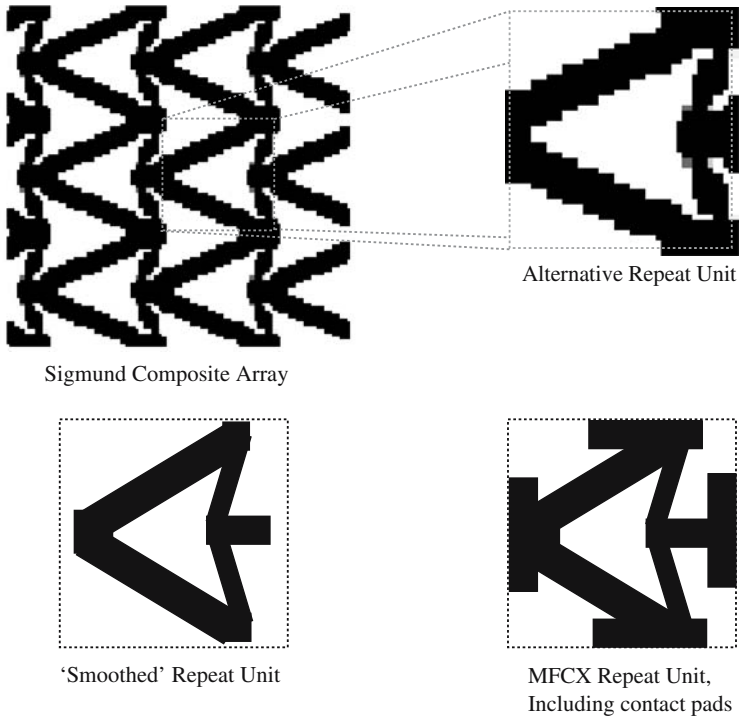

Fig. 7 Negative Poisson's ratio repeat unit modified to facilitate MFCX process

had a gauge length of 4.5 cm, was tested to failure at a strain rate of 0.4×10^{-4}/s. The ultimate tensile strength (UTS) was 340 MPa, and ductility was12%. This is consistent with values for wrought 99% pure nickel, which is typically UTS 317 MPa and 30% ductility [20]. The lower ductility can be attributed to residual porosity. These results show that it is possible to create quality metallic nickel from nickel oxide powder. No deleterious effects were observed during any of the processing steps including green forming, binder burnout, metal oxide reduction or metallic sintering.

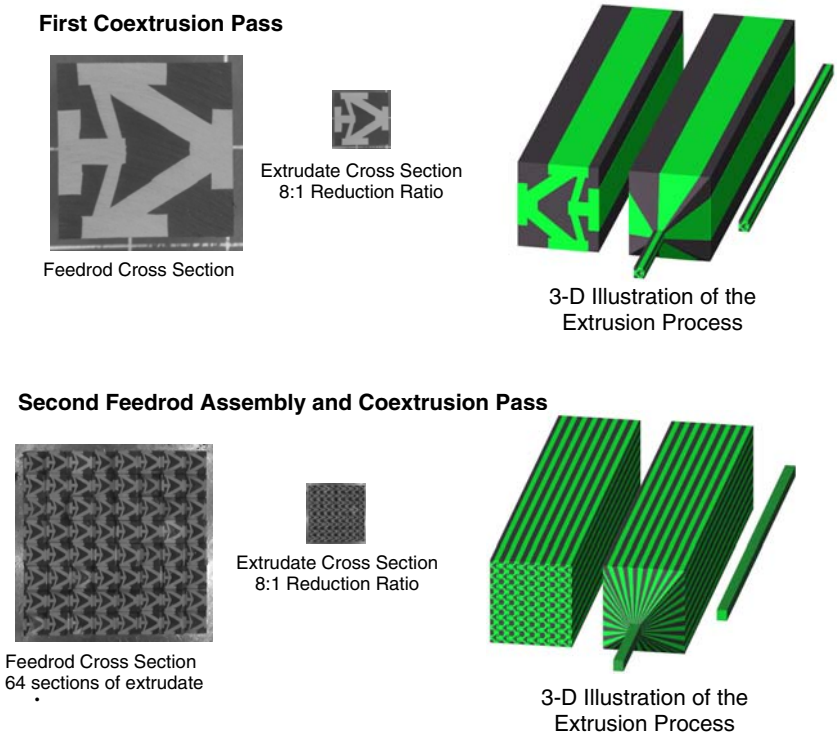

Fig. 8 Coextrusion Process for Ni Negative Poisson's Ratio Object Left: First Feedrod with one repeat unit 38-mm square (top) to be reduced 8:1 in first coextrusion pass to produce 4.75 mm extrudate. Second Feedrod assembled from 64 extruded pieces to be reduced again by 8:1 in second coextrusion pass to produce 4.75 mm extrudate with 64 bonded units, each 594 μm tall Right: 3-D drawings illustrating extrusion process

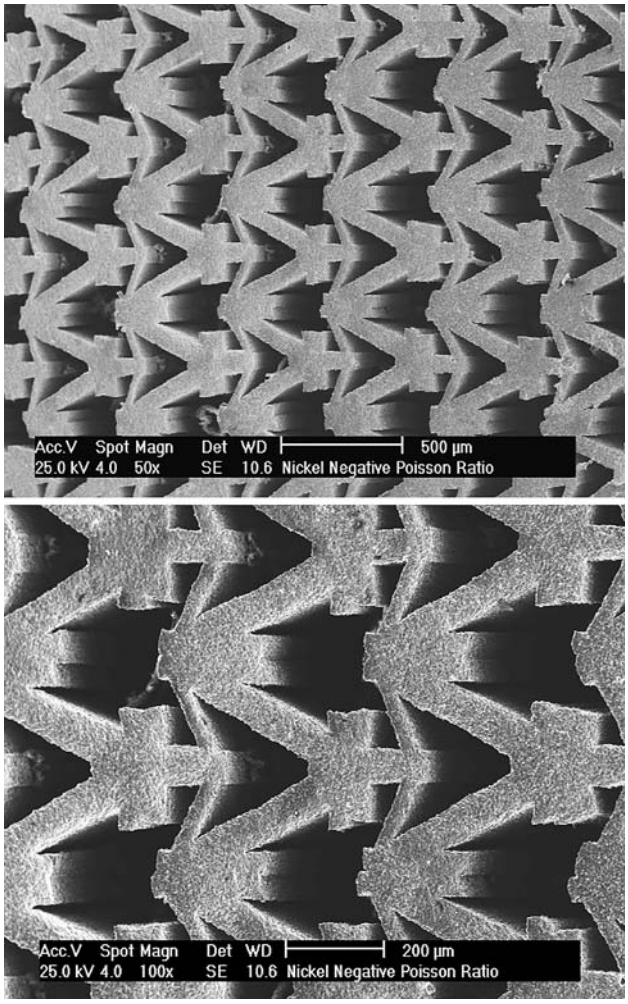

Fig. 9 SEM images of the open channeled metallic nickel negative Poisson's ratio structure

Nickel negative Poisson's ratio structure fabrication

Fabricating the zirconia ceramic showed that registration of the repeat units could be difficult, so the design was modified. Figure 7 shows the modification of the design with an alternate repeat unit which is easier the coextrusion process. The angled struts were smoothed while maintaining their relative positions, angles and volumes. Contact pads were added at the borders of the repeat unit to ensure proper registration between neighboring repeat units. Figure 8 illustrates the coextrusion processing. The upper left is a photograph of the cross section of the first feed rod. The feed rod was coextruded twice through an 8:1 square reduction die at 3 mm/min and during both coextrusion passes and the architecture of the final extrudate material exhibited excellent agreement with the original modified repeat unit design.

Sections were sliced from extrudate using a sharp blade. The green parts were placed on a powder bed of dead burned alumina. Binder burnout and fugitive removal was accomplished by thermally processing in a flowing air atmosphere according to the following schedule; 90 °C/h to 170 °C with a 0.1 h hold, 5 °C/h to 225 °C with a 1.0 h hold, 4 °C/h to 265 °C with a 1.0 h hold, 8 °C/h to 325 °C with a 1.0 h hold, 20 °C/h to 400 °C with a 0.5 h hold, and 60 °C/h to 650 °C with a 0.1 h hold. The binderless parts were furnace cooled. Nickel oxide reduction and sintering was achieved in an atmosphere controlled tube furnace under flowing $10\%H_2/90\%N_2$ reduction gas. After allowing sufficient time to flush any residual air from the system, the part were simultaneously reduced and sintered by heating at 90 °C/h to 1,050 °C with a 1.5 h hold. The metallic parts were furnace cooled under the reducing atmosphere. Images of the metallic nickel negative Poisson's ratio object are shown in Fig. 9, showing that final object is an array of 64 well-bonded repeat units, each 400 µm in size and composed of individual struts and joints with a minimum feature size of 50 µm.

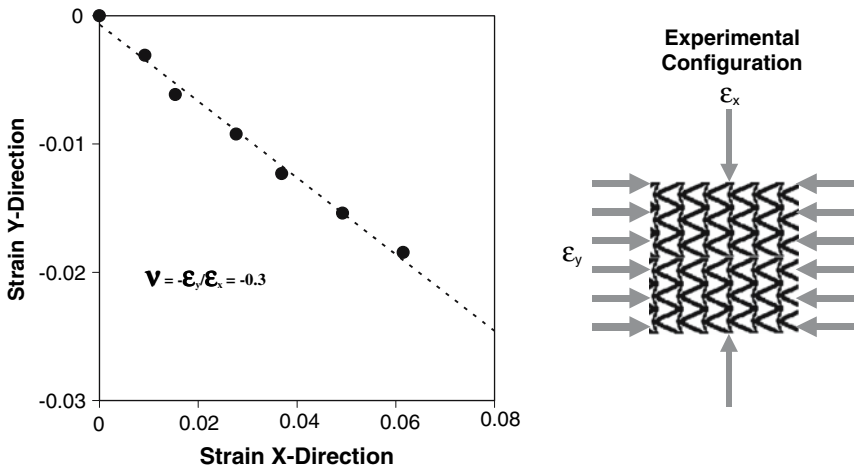

Fig. 10 Testing geometry and Poisson's ratio measurement results for metallic nickel negative Poisson's ratio architecture samples

Determination of Poisson's ratio

Samples of negative Poisson's ratio material were tested using a precision linear displacement stage to load the sample in compression at precise strain intervals while simultaneously measuring the displacement orthogonal direction using a fiber optic displacement probe (Philtec Fiber Optic Probe, USA). The test setup geometry is indicated in the drawing inset into the plot of the results in Fig. 10. A linear fit of the strain in the *y* direction versus strain in the *x* direction yielded a Poisson's ratio of a negative 0.3. This value deviates significantly from the theoretical value of a negative 0.67 specified by the Sigmund's design. The negative Poisson's ratio structure is a type of compliant mechanism that uses discrete flexure joints to approximate pin joints [21, 22]. The architectural approximations made during the feed rod forming process replaced the two discrete compliant hinge points in the original design by a thin flexible beam in the feed rod assembly (distributed compliant hinge) and the junction of the two largest beams was reinforced in the assembled feed rod. The deviations highlighted in the figure are more than likely responsible for the discrepancy between theoretical and experimental negative Poisson's ratio values.

Conclusions

The microfabrication by coextrusion process was used to create a negative Poisson's ratio architecture was from zirconia. However the brittle nature of the ceramic coupled with the poor registration between neighboring repeat units made it difficult to measure the elastic properties. A second attempt was made to construct the same negative Poisson's ratio architecture using nickel oxide. A reducing atmosphere was used to transform nickel oxide into its metallic form after pyrolysis of polymeric binders and fugitive powder. The final nickel object exhibited an experimentally determined Poisson's ratio value of –0.3. The lack of agreement between the –0.67 value predicted by the topology optimization process is believed to be attributed to architectural deviations between the theoretical design and the fabricated object.

Acknowledgement The authors thank the Office of Naval Research and Dr. Stephen Fishman for support.

References

1. Haeri AY, Weidner DJ, Parise JB (1992) Science 257:650
2. Gibson L, Ashby M (1997) Cellular solids, 2nd edn. Cambridge University Press, Cambridge, p 187
3. Lakes R (1987) Science 235:1038
4. Friis E, Lakes R, Park J (1988) J Mater Sci 23:4406
5. Neale PJ, Alderson KL, Pickles AP, Evans KE (1993) J Mater Sci Lett 12:1529
6. Caddock BD, Evans KE (1989) J Phys D Appl Phys 22:1877
7. Caddock BD, Evans KE (1989) J Phys D Appl Phys 22:1883
8. He CL, Puwei G, Anselm C (1998) Macromolecules 31:3145
9. Freedman A (1990) J Sound Vibrat 137:209
10. Nkansah MA, Evans KE, Hutchinson IJ (1993) J Mater Sci 28:2687
11. Choi JB, Lakes RS (1991) Cell Polymer 10:205
12. Choi JB, Lakes RS (1992) J Mater Sci 27:4678
13. Choi JB, Lakes RS (1992) J Mater Sci 27:5372
14. Fonseca JSO (1997) Design of microstructures of periodic composite materials. PhD Thesis, University of Michigan, Department of Mechanical Engineering and Applied Mechanics
15. Sigmund O (1995) Mechanics Mater 20:351
16. Larsen U, Sigmund O, Bouwstra S (1997) J Microelectromechanical Syst 6:99
17. Van Hoy C, Barda A, Griffith ML, Halloran JW (1998) J Am Ceramic Soc 81:152
18. Crumm AT, Halloran JW (1998) J Am Ceramic Soc 81:1053
19. German RM (1984) Powder metallurgy science, 2nd edn. Metal Powder Industries Federation, Princeton, NJ, p 95
20. Davis JR (ed) (1998) Metals handbook – desk edition, 2nd edn. ASM International, Materials Park, OH, p 609
21. Frecker M, Ananthasuresh G, Nishiwaki S, Kikuchi N, Kota S (1997) J Mech Des 119:238
22. Saggere L, Kota S (1999) AIAA J 37:572